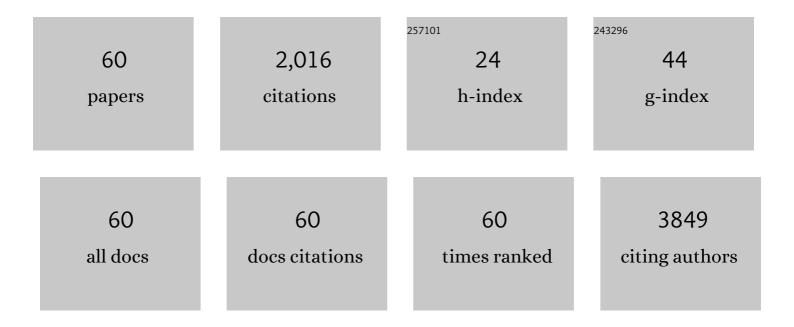
Alexander S Walton

List of Publications by Year in descending order

Source: https://exaly.com/author-pdf/3931539/publications.pdf Version: 2024-02-01



#	Article	IF	CITATIONS
1	Nanostructured Aptamer-Functionalized Black Phosphorus Sensing Platform for Label-Free Detection of Myoglobin, a Cardiovascular Disease Biomarker. ACS Applied Materials & Interfaces, 2016, 8, 22860-22868.	4.0	208
2	<i>In Situ</i> Detection of Active Edge Sites in Single-Layer MoS ₂ Catalysts. ACS Nano, 2015, 9, 9322-9330.	7.3	144
3	Structure and Electronic Properties of <i>In Situ</i> Synthesized Single-Layer MoS ₂ on a Gold Surface. ACS Nano, 2014, 8, 6788-6796.	7.3	136
4	Synthesis of High‣urfaceâ€Area Platinum Nanotubes Using a Viral Template. Advanced Functional Materials, 2010, 20, 1295-1300.	7.8	118
5	Edge reactivity and water-assisted dissociation on cobalt oxide nanoislands. Nature Communications, 2017, 8, 14169.	5.8	117
6	MoS2 nanoparticle morphologies in hydrodesulfurization catalysis studied by scanning tunneling microscopy. Journal of Catalysis, 2013, 308, 306-318.	3.1	101
7	Ambient-air-stable inorganic Cs ₂ Snl ₆ double perovskite thin films <i>via</i> aerosol-assisted chemical vapour deposition. Journal of Materials Chemistry A, 2018, 6, 11205-11214.	5.2	85
8	Interface Controlled Oxidation States in Layered Cobalt Oxide Nanoislands on Gold. ACS Nano, 2015, 9, 2445-2453.	7.3	78
9	In situ investigation of degradation at organometal halide perovskite surfaces by X-ray photoelectron spectroscopy at realistic water vapour pressure. Chemical Communications, 2017, 53, 5231-5234.	2.2	78
10	Four-probe electrical transport measurements on individual metallic nanowires. Nanotechnology, 2007, 18, 065204.	1.3	71
11	Origin of significant visible-light absorption properties of Mn-doped TiO2 thin films. Acta Materialia, 2012, 60, 1974-1985.	3.8	56
12	Investigation of the Differential Capacitance of Highly Ordered Pyrolytic Graphite as a Model Material of Graphene. Langmuir, 2016, 32, 11448-11455.	1.6	43
13	Factors that determine and limit the resistivity of high-quality individual ZnO nanowires. Nanotechnology, 2013, 24, 435706.	1.3	39
14	Gold-supported two-dimensional cobalt oxyhydroxide (CoOOH) and multilayer cobalt oxide islands. Physical Chemistry Chemical Physics, 2017, 19, 2425-2433.	1.3	38
15	Oleylamine Aging of PtNi Nanoparticles Giving Enhanced Functionality for the Oxygen Reduction Reaction. Nano Letters, 2021, 21, 3989-3996.	4.5	37
16	Vanadium(iii) phenoxyimine complexes for ethylene or ε-caprolactone polymerization: mononuclear versus binuclear pre-catalysts. Catalysis Science and Technology, 2013, 3, 152-160.	2.1	36
17	Understanding the CO Oxidation on Pt Nanoparticles Supported on MOFs by <i>Operando</i> XPS. ChemCatChem, 2018, 10, 4238-4242.	1.8	35
18	Controlling the Electrical Transport Properties of Nanocontacts to Nanowires. Nano Letters, 2015, 15, 4248-4254.	4.5	34

ALEXANDER S WALTON

#	Article	IF	CITATIONS
19	Four-probe electrical characterization of Pt-coated TMV-based nanostructures. Nanotechnology, 2008, 19, 165704.	1.3	32
20	Low-Temperature Preparation of Single Crystal Titanium Carbide Nanofibers in Molten Salts. Crystal Growth and Design, 2011, 11, 3122-3129.	1.4	30
21	Comparative Analysis of Cobalt Oxide Nanoisland Stability and Edge Structures on Three Related Noble Metal Surfaces: Au(111), Pt(111) and Ag(111). Topics in Catalysis, 2017, 60, 503-512.	1.3	29
22	Vanadyl calix[6]arene complexes: synthesis, structural studies and ethylene homo-(co-)polymerization capability. Dalton Transactions, 2015, 44, 12292-12303.	1.6	27
23	Phase Transitions of Cobalt Oxide Bilayers on Au(111) and Pt(111): The Role of Edge Sites and Substrate Interactions. Journal of Physical Chemistry B, 2018, 122, 561-571.	1.2	26
24	Use of titanocalix[4]arenes in the ring opening polymerization of cyclic esters. Catalysis Science and Technology, 2020, 10, 1619-1639.	2.1	25
25	Optical Study of p-Doping in GaAs Nanowires for Low-Threshold and High-Yield Lasing. Nano Letters, 2019, 19, 362-368.	4.5	24
26	An investigation of the growth of bismuth whiskers and nanowires during physical vapour deposition. Journal Physics D: Applied Physics, 2012, 45, 435304.	1.3	22
27	Highly Active, Thermally Stable, Ethylene-Polymerisation Pre-Catalysts Based on Niobium/Tantalumlmine Systems. Chemistry - A European Journal, 2013, 19, 8884-8899.	1.7	22
28	Zirconium as a Boron Sink in Crystalline CoFeB/MgO/CoFeB Magnetic Tunnel Junctions. Applied Physics Express, 2011, 4, 013002.	1.1	19
29	The offset droplet: a new methodology for studying the solid/water interface using x-ray photoelectron spectroscopy. Journal of Physics Condensed Matter, 2017, 29, 454001.	0.7	17
30	Formation of a U(VI)–Persulfide Complex during Environmentally Relevant Sulfidation of Iron (Oxyhydr)oxides. Environmental Science & Technology, 2020, 54, 129-136.	4.6	17
31	Room-Temperature Production of Nanocrystalline Molybdenum Disulfide (MoS ₂) at the Liquidâ^'Liquid Interface. Chemistry of Materials, 2019, 31, 5384-5391.	3.2	16
32	Role of Alkali Cations in Stabilizing Mixed-Cation Perovskites to Thermal Stress and Moisture Conditions. ACS Applied Materials & Interfaces, 2021, 13, 43573-43586.	4.0	16
33	An Exemplar Imidazoline Surfactant for Corrosion Inhibitor Studies: Synthesis, Characterization, and Physicochemical Properties. Journal of Surfactants and Detergents, 2020, 23, 225-234.	1.0	15
34	Hydrogenation of benzoic acid to benzyl alcohol over Pt/SnO2. Applied Catalysis A: General, 2020, 593, 117420.	2.2	15
35	Modulating Crystallization in Semitransparent Perovskite Films Using Submicrometer Spongelike Polymer Colloid Particles to Improve Solar Cell Performance. ACS Applied Energy Materials, 2019, 2, 6624-6633.	2.5	14
36	Structure and Stability of Au-Supported Layered Cobalt Oxide Nanoislands in Ambient Conditions. Journal of Physical Chemistry C, 2019, 123, 9176-9182.	1.5	14

ALEXANDER S WALTON

#	Article	IF	CITATIONS
37	Photoelectric Properties of Electrodeposited Copper(I) Oxide Nanowires. Journal of the Electrochemical Society, 2009, 156, K191.	1.3	13
38	Air-Stable Methylammonium Lead Iodide Perovskite Thin Films Fabricated via Aerosol-Assisted Chemical Vapor Deposition from a Pseudohalide Pb(SCN) ₂ Precursor. ACS Applied Energy Materials, 2019, 2, 6012-6022.	2.5	13
39	Nanoscale Chevrel-Phase Mo ₆ S ₈ Prepared by a Molecular Precursor Approach for Highly Efficient Electrocatalysis of the Hydrogen Evolution Reaction in Acidic Media. ACS Applied Energy Materials, 2021, 4, 13015-13026.	2.5	12
40	Magnetic field enhanced nano-tip fabrication for four-probe STM studies. Nanotechnology, 2008, 19, 085201.	1.3	11
41	ZnO nanowires with Au contacts characterised in the as-grown real device configuration using a local multi-probe method. Nanotechnology, 2014, 25, 425706.	1.3	11
42	Adsorption site, orientation and alignment of NO adsorbed on Au(100) using 3D-velocity map imaging, X-ray photoelectron spectroscopy and density functional theory. Physical Chemistry Chemical Physics, 2019, 21, 10939-10946.	1.3	11
43	Patchiness of ion-exchanged mica revealed by DNA binding dynamics at short length scales. Nanotechnology, 2014, 25, 025704.	1.3	10
44	Intercalation, decomposition, entrapment – a new route to graphene nanobubbles. Physical Chemistry Chemical Physics, 2020, 22, 7606-7615.	1.3	10
45	Decoupling Structure and Composition of CH ₃ NH ₃ PbI _{3–<i>x</i>} Br _{<i>x</i>} Films Prepared by Combined One-Step and Two-Step Deposition. ACS Applied Energy Materials, 2018, 1, 5567-5578.	2.5	9
46	Intrinsic effects of thickness, surface chemistry and electroactive area on nanostructured MoS2 electrodes with superior stability for hydrogen evolution. Electrochimica Acta, 2021, 382, 138257.	2.6	9
47	High-Performance Nanostructured MoS ₂ Electrodes with Spontaneous Ultralow Gold Loading for Hydrogen Evolution. Journal of Physical Chemistry C, 2021, 125, 20940-20951.	1.5	9
48	Universal shape of graphene nanobubbles on metallic substrate. Physical Chemistry Chemical Physics, 2022, 24, 6935-6940.	1.3	9
49	Nanocubes of Mo ₆ S ₈ Chevrel phase as active electrode material for aqueous lithium-ion batteries. Nanoscale, 2022, 14, 10125-10135.	2.8	9
50	Water-induced reordering in ultrathin ionic liquid films. Journal of Physics Condensed Matter, 2018, 30, 334003.	0.7	8
51	PtNi bimetallic structure supported on UiO-67 metal-organic framework (MOF) during CO oxidation. Journal of Catalysis, 2020, 391, 522-529.	3.1	7
52	Direct <i>in situ</i> spectroscopic evidence of the crucial role played by surface oxygen vacancies in the O ₂ -sensing mechanism of SnO ₂ . Chemical Science, 2022, 13, 6089-6097.	3.7	7
53	Core level photoemission line shape selection: Atomic adsorbates on iron. Surface and Interface Analysis, 2020, 52, 507-512.	0.8	6
54	A combined laboratory and synchrotron in-situ photoemission study of the rutile TiO ₂ (110)/water interface. Journal Physics D: Applied Physics, 2021, 54, 194001.	1.3	6

ALEXANDER S WALTON

#	Article	IF	CITATIONS
55	Corrosion inhibition in acidic environments: key interfacial insights with photoelectron spectroscopy. Faraday Discussions, 2022, 236, 374-388.	1.6	6
56	Reversible metallisation of soft UV patterned substrates. Journal of Materials Chemistry C, 2014, 2, 5916-5923.	2.7	4
57	Photo-Seebeck study of amorphous germanium–tellurium-oxide films. Journal of Materials Science: Materials in Electronics, 2020, 31, 22000-22011.	1.1	1
58	Manipulation of Molecular Vibrations on Condensing Er3+ State Densities for 1.5 $\hat{l}^1\!/4$ m Application. Journal of Physical Chemistry Letters, 2021, 12, 9620-9625.	2.1	1
59	Evaporation and decomposition of acrylic acid grafted luminescent silicon quantum dots in ultrahigh vacuum. Journal of Physics: Conference Series, 2011, 286, 012039.	0.3	Ο
60	Examining the crystal growth that influences the electronic device output from vertical arrays of ZnO nanowires. Materials Research Society Symposia Proceedings, 2014, 1659, 101-106.	0.1	0